

# B Mixing and Lifetimes at the Tevatron

G. Gómez-Ceballos

*Instituto de Física de Cantabria (CSIC-UC), Avda. de los Castros s/n, 39005 Santander, Spain*

J. Piedra

*LPNHE-IN2P3/CNRS, Universites Paris VI et Paris VII, 4 Place Jussieu Tour 33, 75252 Paris, France*

The Tevatron collider at Fermilab provides a very rich environment for the study of  $b$ -hadrons. Both the DØ and CDF experiments have collected a sample of about  $1 \text{ fb}^{-1}$ . We report results on three topics:  $b$ -hadron lifetimes, polarization amplitudes and the decay width difference in  $B_s^0 \rightarrow J/\psi\phi$ , and  $B_s^0$  mixing.

## 1. Introduction

The Tevatron collider at Fermilab, operating at  $\sqrt{s} = 1.96 \text{ TeV}$ , has a huge  $b\bar{b}$  production cross section which is several orders of magnitude larger than the production rate at  $e^+e^-$  colliders running on the  $\Upsilon(4S)$  resonance. In addition, on the  $\Upsilon(4S)$  only  $B^+$  and  $B_d^0$  are produced, while higher mass  $b$ -hadrons such as  $B_s^0$ ,  $B_c$ ,  $b$ -baryons,  $B^*$ , and  $p$ -wave  $B$  mesons are currently produced only at the Tevatron.

Both DØ and CDF II are multipurpose detectors featuring high resolution tracking in a magnetic field and lepton identification. These detectors are symmetrical in polar and azimuthal angles around the interaction point, with approximate  $4\pi$  coverage [1, 2]. The CDF II and DØ detectors are able to trigger at the hardware level on large track impact parameters, enhancing the potential of their  $B$  physics programs.

## 2. Precision Lifetimes

The lifetime of  $b$ -hadrons is governed primarily by the decay of the  $b$ -quark, however contributions from the spectator quarks introduce small differences between the lifetimes of different species. Presently these spectator effects are mostly calculated in the framework of the Heavy Quark Expansion [3].

Several new results have been obtained by DØ and CDF, most of them already included in the world averages, and summarized in Table I [4]. The lifetime of the  $\Lambda_b^0$  baryon has been determined by both experiments through the  $\Lambda_b^0 \rightarrow J/\psi\Lambda^0$  decay,

$$\tau_{\Lambda_b^0}^{DØ} = 1.22_{-0.18}^{+0.22} \text{ (stat.)} \pm 0.04 \text{ (syst.) ps [250 pb}^{-1}\text{]},$$

$$\tau_{\Lambda_b^0}^{CDF} = 1.593_{-0.078}^{+0.083} \text{ (stat.)} \pm 0.033 \text{ (syst.) ps [1 fb}^{-1}\text{]}.$$

Previous results used semileptonic  $\Lambda_b^0 \rightarrow \Lambda_c^+ \ell^- \bar{\nu}_\ell$  decays. Fully reconstructed decays are preferable because they do not suffer from possible unexpected contributions from other  $b$ -baryon decays, and do not require a correction for the missing momentum from unreconstructed decay products (*e.g.*, the neutrino). The CDF measured value of  $\tau_{\Lambda_b^0}$  is  $3.1\sigma$  higher than

the current world average [5]. This is the most precise single measurement of  $\tau_{\Lambda_b^0}$ . The fit projections of both lifetime measurements can be seen in Fig. 1.

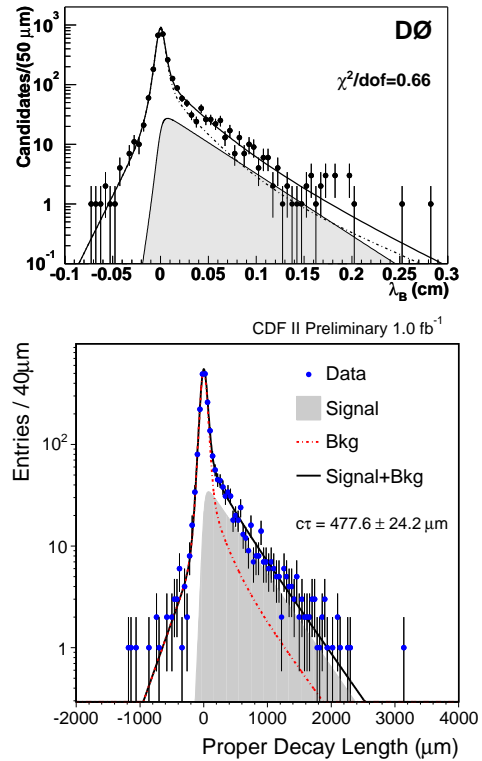


Figure 1: Lifetime results from the  $\Lambda_b^0 \rightarrow J/\psi\Lambda^0$  decay. The points are the data, and the solid curve is the sum of fitted contributions from signal (shaded area) and background (dot-dashed line).

In the case of the  $B_s^0$  meson, the lifetime is extracted from the semileptonic decay  $B_s^0 \rightarrow D_s^- \ell^+ \nu$ , providing the world's best measurement from DØ [6],

$$\tau_{B_s^0}^{DØ} = 1.398 \pm 0.044 \text{ (stat.)}_{-0.025}^{+0.028} \text{ (syst.) ps [400 pb}^{-1}\text{]},$$

$$\tau_{B_s^0}^{CDF} = 1.381 \pm 0.055 \text{ (stat.)}_{-0.046}^{+0.052} \text{ (syst.) ps [370 pb}^{-1}\text{]}.$$

Table I HFAG March 2006 averages compared to theory calculations.

<i>b</i> -hadron species	lifetime [ps]	$\tau/\tau(B_d^0)$	
		average	predicted range
$B^+$	$1.643 \pm 0.010$	$1.076 \pm 0.008$	1.04 – 1.08
$B_s^0$	$1.454 \pm 0.040$	$0.914 \pm 0.030$	0.99 – 1.01
$\Lambda_b^0$	$1.288 \pm 0.065$	$0.844 \pm 0.043$	0.86 – 0.95
$B_d^0$	$1.527 \pm 0.008$	—	—
$B_c$	$0.469 \pm 0.065$	—	—

### 3. Polarization Amplitudes

The heavy  $B_s^H$  and light  $B_s^L$  mass eigenstates of the  $B_s^0$  meson are mixtures of the two  $CP$ -conjugate states. Due to this mixture, the masses and lifetimes of the mass eigenstates differ:

$$\Delta m \equiv m_H - m_L, \quad \Delta \Gamma \equiv \Gamma_L - \Gamma_H, \quad (1)$$

where  $m_{H,L}$  and  $\Gamma_{H,L}$  denote the  $B_s^{H,L}$  mass and decay width. One of the important goals in Run II is to measure the lifetime difference  $\Delta \Gamma$  between these two mass eigenstates. They are expected to be  $CP$  eigenstates if the mixing phase is small. As it has been shown theoretically [7], an angular analysis based on transversity variables, combined with a lifetime measurement, permits one to separate the  $CP$ -even and  $CP$ -odd final states of  $B_s^0 \rightarrow J/\psi \phi$  (with  $J/\psi \rightarrow \mu^+ \mu^-$  and  $\phi \rightarrow K^+ K^-$ ), and hence determine the lifetime difference.

Based on the single muon trigger, the DØ experiment analyzes  $0.8 \text{ fb}^{-1}$ , with  $978 \pm 45 B_s^0$  candidates passing the selection cuts. A simultaneous unbinned likelihood fit is performed in terms of invariant mass, proper decay length and transversity angular variables, described in [8]. Due to limited detector coverage and kinematic thresholds, the detector response to the transversity angles is non-uniform. The acceptance is modelled with Monte Carlo simulation, reweighing the simulated events to match the kinematic distributions observed in data.

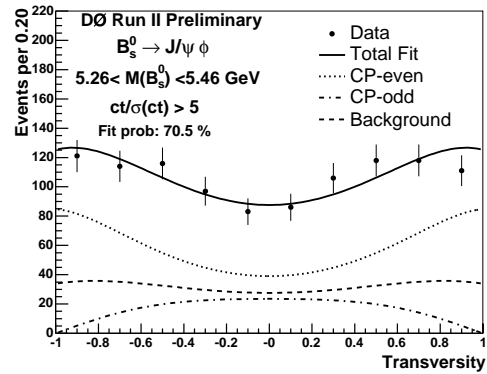
In Fig. 2 we show the projection of the fit result onto the  $\cos \theta$  transversity variable. Similar agreement is observed in the projections onto the invariant mass, proper decay length and remaining transversity angles. The results are presented in Table II. The  $1\sigma$  contour for  $\Delta \Gamma$  versus  $c\bar{\tau}$ , with  $\bar{\tau} = 1/\Gamma = 2/(\Gamma_H + \Gamma_L)$ , is shown in Fig. 3.

### 4. B Mixing

The mixing and  $CP$  violation parameters of  $B$  mesons are currently the focus of much attention for

Table II Tevatron direct measurements of the decay rate difference between the  $B_s^0$  mass eigenstates  $\Delta \Gamma$ , the average lifetime  $\bar{\tau}$ , the fraction of the  $CP$ -odd component at  $t = 0$ ,  $R_\perp = |A_\perp(0)|^2$ , the difference in quadrature of the  $CP$ -even linear polarization amplitude at  $t = 0$ ,  $|A_0(0)|^2 - |A_\parallel(0)|^2$ , and the difference of the two  $CP$ -conserving strong phases  $\delta_1 - \delta_2$ . The  $CP$ -violating weak phase is assumed to be zero.

observable	CDF '04 [9]	DØ '06 [10]
$\Delta \Gamma$ [ $\text{ps}^{-1}$ ]	$0.47^{+0.19}_{-0.24} \pm 0.01$	$0.15^{+0.10+0.03}_{-0.10-0.04}$
$\bar{\tau}$ [ps]	$1.40^{+0.15}_{-0.13}$	$1.53^{+0.08+0.01}_{-0.08-0.04}$
$R_\perp$	$0.13 \pm 0.08$	$0.19 \pm 0.05 \pm 0.01$
$ A_0(0) ^2 -  A_\parallel(0) ^2$	$0.355 \pm 0.067$	$0.35 \pm 0.07 \pm 0.01$
$\delta_1 - \delta_2$	$1.94 \pm 0.36$	$2.5 \pm 0.4$

Figure 2:  $\cos \theta$  transversity distribution (DØ). The curves show: total fit (solid line),  $CP$ -even (dotted line),  $CP$ -odd (dot-dashed line) and background (dashed line).

pinning down the CKM matrix, and perhaps exposing new physics beyond the Standard Model. The probability  $\mathcal{P}$  for a  $B_s^0$  meson produced at time  $t = 0$  to decay as  $B_s^0$  ( $\bar{B}_s^0$ ) at proper time  $t > 0$  is, neglecting effects from  $CP$  violation as well as a possible lifetime difference between the heavy and light  $B_s^0$  mass eigenstates,

$$\mathcal{P}_\pm(t) = \frac{\Gamma}{2} e^{-\Gamma t} [1 \pm \cos(\Delta m_s t)], \quad (2)$$

where the subscript “+” (“−”) indicates that the meson decays as  $B_s^0$  ( $\bar{B}_s^0$ ). Oscillations have been observed and well established in the  $B_d^0$  system. The mass difference  $\Delta m_d$  is measured to be [5]

$$\Delta m_d = 0.505 \pm 0.005 \text{ ps}^{-1}.$$

In the  $B_s^0$  system oscillations have also been well established. Time-integrated measurements indicate that  $B_s^0$  mixing is large, with a value of  $\chi_s$  [4] close to its maximal possible value of  $1/2$ ,

$$\chi_s = \frac{x_s^2 + y_s^2}{2(x_s^2 + 1)} > 0.49904 \text{ at } 95\% \text{ C.L.},$$

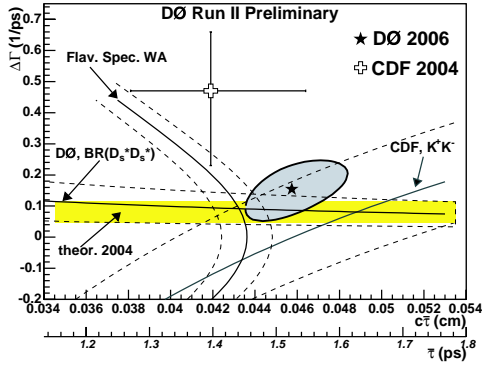


Figure 3: The  $D\bar{0}$   $1\sigma$  (stat.) contour in  $\Delta\Gamma$  versus  $c\bar{\tau}$  plane [10], compared to a  $1\sigma$  band for the world average based on flavor-specific decays [5]. The SM prediction [11] is shown as the horizontal band. Also shown are the CDF 2004 result [9], the recent CDF measurement of the  $B_s^0$  lifetime from the  $B_s^0 \rightarrow K^+K^-$  decay [12], and the implication of the  $D\bar{0}$  result [13] of the branching fraction for the  $B_s^0 \rightarrow D_s^{(*)+}D_s^{(*)-}$  decay.

$$2y_s = \frac{\Delta\Gamma}{\Gamma} = 0.31_{-0.11}^{+0.10}, \quad (3)$$

$$x_s = \frac{\Delta m_s}{\Gamma} > 22.4 \text{ at } 95\% \text{ C.L.}$$

However, the time dependence of this mixing has not been observed yet, and previous attempts to measure  $\Delta m_s$  have yielded a lower limit:  $\Delta m_s > 14.5 \text{ ps}^{-1}$  [5] at the 95% confidence level (C.L.).

The canonical  $B$  mixing analysis proceeds as follows. The  $b$ -flavor ( $b$  or  $\bar{b}$ ) of the  $B$  meson at the time of decay is determined from the charges of the reconstructed decay products in the final state. The proper time at which the decay occurred is determined from the displacement of the  $B_s^0$  decay vertex with respect to the primary vertex, and the  $B_s^0$  transverse momentum with respect to the proton beam. Finally, the production  $b$ -flavor must be known in order to classify the  $B$  meson as being mixed (production and decay  $b$ -flavor are different) or unmixed (production and decay  $b$ -flavor are equal) at the time of its decay.

## 4.1. Signal Yields

Both  $D\bar{0}$  and CDF have performed mixing analyses using  $1 \text{ fb}^{-1}$  of data [14, 15]. The  $D\bar{0}$  experiment exploits the high statistics single muon trigger to study  $B_s^0 \rightarrow \mu^+D_s^-X$ ,  $D_s^- \rightarrow \phi\pi^-$  decays, reconstructing 26,700 signal candidates. On the CDF side, the analysis is performed using both fully reconstructed  $B_s^0 \rightarrow D_s^-(\pi^+\pi^-)\pi^+$  and semileptonic  $B_s^0 \rightarrow \ell^+D_s^-X$  ( $\ell = e, \mu$ ) decays. In both cases the  $D_s^-$  is reconstructed in the  $D_s^- \rightarrow \phi\pi^-$ ,  $D_s^- \rightarrow K^{*0}K^-$  and  $D_s^- \rightarrow \pi^+\pi^-\pi^-$  modes. The signal yields are 3,600 (fully reconstructed) and 37,000 (semileptonic).

Fig. 4 (Fig. 5) shows the reconstructed candidates from  $D\bar{0}$  (CDF).

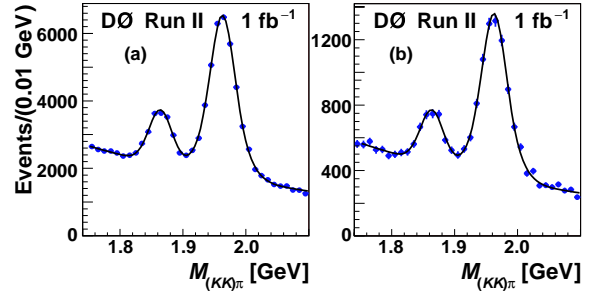


Figure 4:  $(K^+K^-)\pi^-$  invariant mass distribution for (a) untagged  $B_s^0$  sample, and (b) flavor-tagged  $B_s^0$  candidates. The left and right peaks correspond to  $\mu^+D^-$  and  $\mu^+D_s^-$  candidates, respectively.

## 4.2. Decay Length Reconstruction

The transverse decay length  $L_{xy}(B)$  is defined as the displacement from the interaction point to the reconstructed  $B$  vertex, in the plane transverse to the proton beam. The  $B$  meson decay time is then given by

$$t = L_{xy}(B) \frac{M_B}{p_T(B)}, \quad (4)$$

where  $M_B$  is the nominal  $B$  mass [5]. In semileptonic decays, the  $B$  meson is not fully reconstructed, and a correction factor has to be included to account for the missing momentum,

$$t = L_{xy}(\ell D) \frac{M_B}{p_T(\ell D)} k, \quad k \equiv \frac{L_{xy}(B)}{L_{xy}(\ell D)} \frac{p_T(\ell D)}{p_T(B)}. \quad (5)$$

The  $k$ -factor distribution is obtained from MC simulation. Both  $D\bar{0}$  and CDF use different  $k$ -factor distributions as a function of the  $\ell D$  mass, as illustrated in Fig. 6.

The determination of the time resolution is a necessary piece of input for derivation of a proper result on  $\Delta m_s$ . The most precise determinations come from lifetime measurements in the exclusively reconstructed modes involving  $J/\psi$  decays. Usually, the time resolution is part of the fitting procedure and is determined in the  $B$  meson sidebands, which contain a large fraction of prompt events. In those prompt  $J/\psi$  candidates, another track from the primary vertex is combined with the  $J/\psi$ , and is ideally suited for measuring the resolution on  $t$  with respect to the primary vertex position. For analyses which rely on samples obtained with a selection that biases the time distribution, these prompt components in the sidebands are greatly reduced, which makes the determination

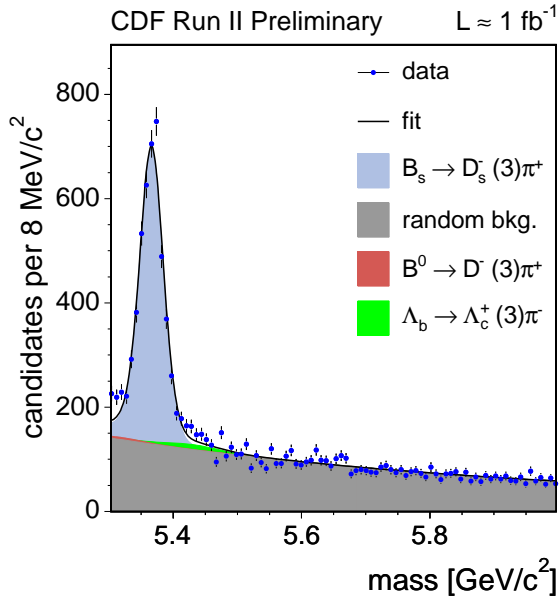
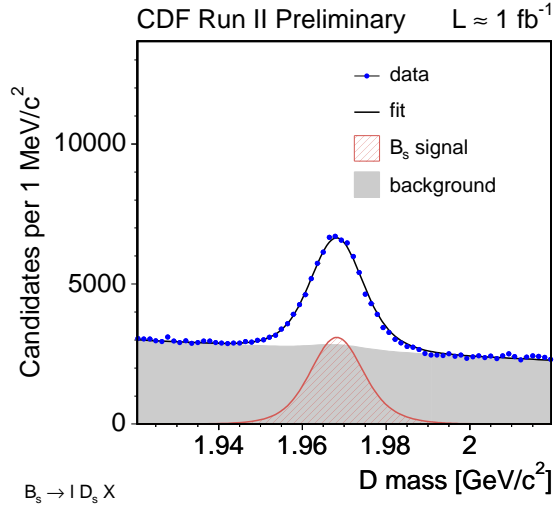


Figure 5:  $D_s^-$  invariant mass distribution for semileptonic decays (top) and  $B_s^0$  invariant mass distribution for fully reconstructed decays (bottom).

of the time resolution problematic. CDF uses unbiased prompt events to measure  $t/\sigma_t$ , and then applies an event-by-event correction, which depends on the decay topology and on several kinematical quantities. DØ uses a sample of  $J/\psi \rightarrow \mu^+\mu^-$  decays to examine the  $t/\sigma_t$  distribution, and then applies an overall correction on the time resolution with a double Gaussian distribution: the narrow Gaussian has a width of  $0.998\sigma$  and comprises 72% of the total, and the second Gaussian has a width of  $2.777\sigma$ , where  $\sigma$  is the estimated error on the proper decay time of the candidate.

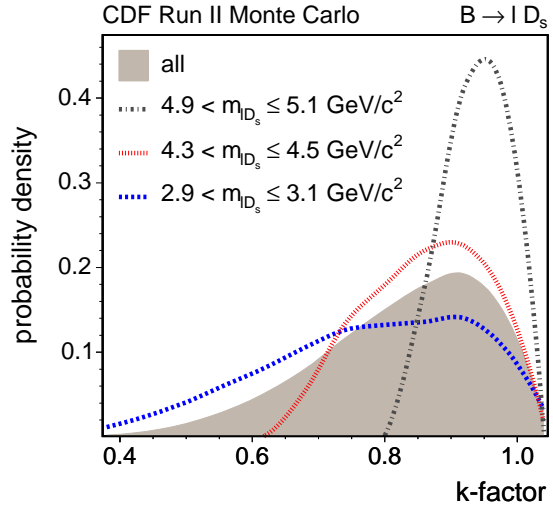


Figure 6:  $k$ -factor distribution for several  $\ell D$  mass regions, for  $B_s^0 \rightarrow \ell^+ D_s^- X$ ,  $D_s^- \rightarrow \phi \pi^-$  decays.

### 4.3. Flavor Tagging

The methods of  $b$ -flavor tagging may be classified into two categories: opposite-side (soft lepton and jet charge) and same-side production  $b$ -flavor identification. Opposite-side taggers exploit the fact that  $b$  quarks in hadron colliders are mostly produced in  $b\bar{b}$  pairs. Same-side flavor tags are based on the charge of particles produced in association with the production of the  $b$ -hadron.

The performance of the  $b$ -flavor taggers is quantified by their efficiency  $\epsilon$  and dilution  $\mathcal{D} = 2P_{tag} - 1$ , where  $P_{tag}$  is the probability for the production  $b$ -flavor to be correctly identified. For setting a limit on  $\Delta m_s$ , knowledge of the flavor taggers performance is crucial.

### 4.4. Opposite-Side Flavor Tagging

The soft lepton tagger (SLT) is based on semileptonic  $b$  decays into an electron or a muon ( $b \rightarrow \ell^- X$ ). The charge of the lepton is correlated to the charge of the decaying  $B$  meson. The jet charge tagger (JQT) uses the fact that the charge of a  $b$ -jet is correlated to the charge of the  $b$  quark.

The performance of the opposite-side flavor taggers is measured in kinematically similar  $B_d^0$  and  $B^+$  samples, and we summarize it in Table III. The analysis involves complex fits combining several  $B_d^0$  and  $B^+$  decay modes. Both DØ and CDF have measured  $\Delta m_d$  and find

$$\Delta m_d^{D\emptyset} = 0.506 \pm 0.020 \text{ (stat.)} \pm 0.016 \text{ (syst.) ps}^{-1},$$

$$\Delta m_d^{CDF} = 0.509 \pm 0.010 \text{ (stat.)} \pm 0.016 \text{ (syst.) ps}^{-1}.$$

Table III Opposite-side flavor taggers performance.

tagger	$\epsilon\mathcal{D}^2$ [%]	
	DØ	CDF
muon	$1.48 \pm 0.17$	$0.55 \pm 0.05$
electron	$0.21 \pm 0.07$	$0.30 \pm 0.03$
JQT	$0.50 \pm 0.11$	$0.70 \pm 0.06$
combined	$2.48 \pm 0.22$	$1.55 \pm 0.08$

## 4.5. Same-Side Flavor Tagging

During the fragmentation and the formation of the  $B_s^0$  meson there is a left over  $\bar{s}$  quark which may form a  $K^+$ . Hence, if there is a nearby charged particle, which is additionally identified as a kaon, it is quite likely that it is the leading fragmentation track and its charge is then correlated to the flavor of the  $B_s^0$  meson. While the performance of an opposite-side tagger does not depend on the flavor of the  $B$  on the signal side, the same-side tagger performance depends on the signal fragmentation process. Therefore the opposite-side performance can be measured in  $B_d^0$  and  $B^+$  samples, and can then be used for setting a limit on the  $B_s^0$  mixing frequency. But when using a same-side tagger for a limit on  $\Delta m_s$ , one must rely on Monte Carlo simulation.

CDF has performed extensive data and Monte Carlo comparisons on several quantities related to the tagging, and determined the tagging candidate by selecting the most likely kaon track. To separate kaons from other particle species, a combined particle identification likelihood based on information from  $dE/dx$  and from the Time-of-Flight system has been used. A comparison between data and PYTHIA Monte Carlo [16] for the dilution obtained by using that likelihood is shown in Fig. 7. There we can see an excellent agreement between the results obtained from Monte Carlo, and those from data, thus providing confidence on the performance description in Monte Carlo. The effectiveness of this flavor tag increases with the  $p_T$  of the  $B_s^0$ . The values found using PYTHIA Monte Carlo are  $\epsilon\mathcal{D}^2 = 3.5\%$  (4.0%) in the hadronic (semileptonic) decay sample.

## 4.6. Amplitude Scan

The likelihood term describing the proper decay time of flavor-tagged neutral  $B$  meson candidates is modified by including an additional parameter multiplying the cosine, the so-called amplitude  $\mathcal{A}$ ,

$$\mathcal{L}_{\text{signal}} \propto 1 \pm \mathcal{A}\mathcal{D} \cos(\Delta mt). \quad (6)$$

The parameter  $\mathcal{A}$  is left free in the fit while  $\mathcal{D}$  is known, as explained in Sec. 4.4 and 4.5, and fixed in the scan. This method [17] involves performing

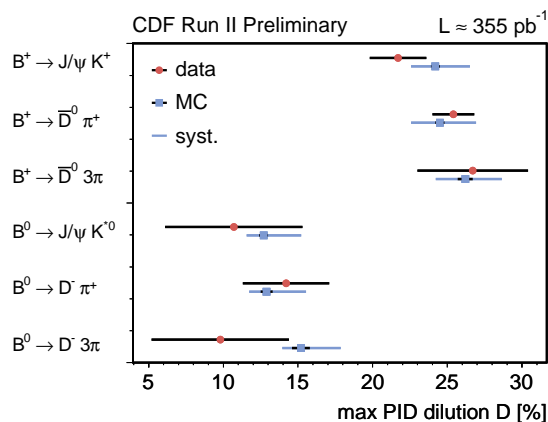


Figure 7: Comparison between CDF data and PYTHIA Monte Carlo for the dilution obtained by selecting the most likely kaon track as the tag.

one such  $\mathcal{A}$ -fit for each value of the parameter  $\Delta m$ , which is fixed at each step; in the case of infinite statistics, optimal resolution and perfect dilution calibration, one would expect  $\mathcal{A}$  to be unity for the true oscillation frequency and zero for the remainder of the probed spectrum. In practice, the output of the procedure is accordingly a list of fitted values ( $\mathcal{A}$ ,  $\sigma_{\mathcal{A}}$ ) for each  $\Delta m$  hypothesis. A particular  $\Delta m$  hypothesis is excluded to a 95% confidence level in case the following relation is observed:  $\mathcal{A} + 1.645\sigma_{\mathcal{A}} < 1$ . The sensitivity of a mixing measurement is defined as the  $\Delta m$  value for which  $1.645\sigma_{\mathcal{A}} = 1$ .

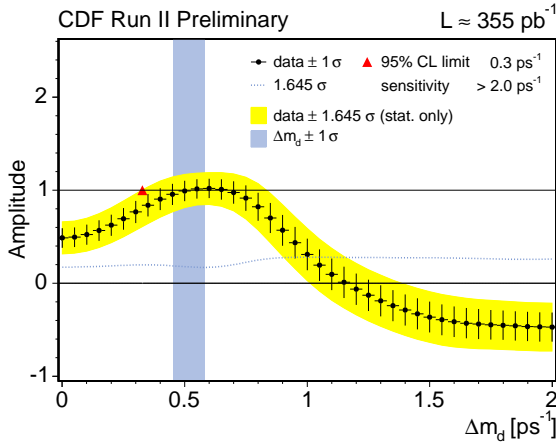
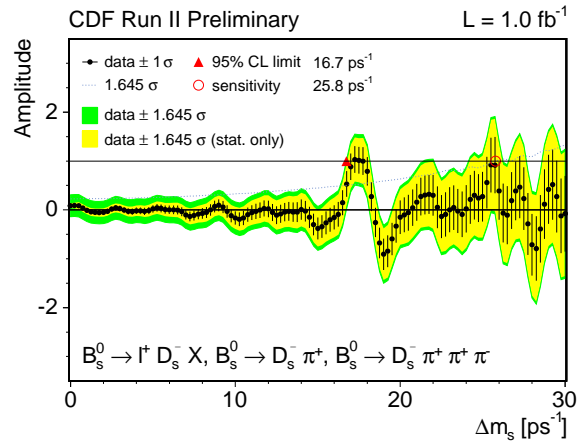
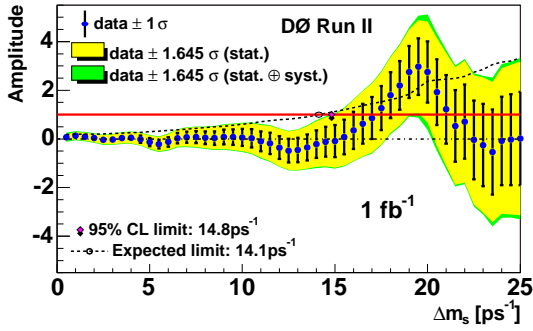
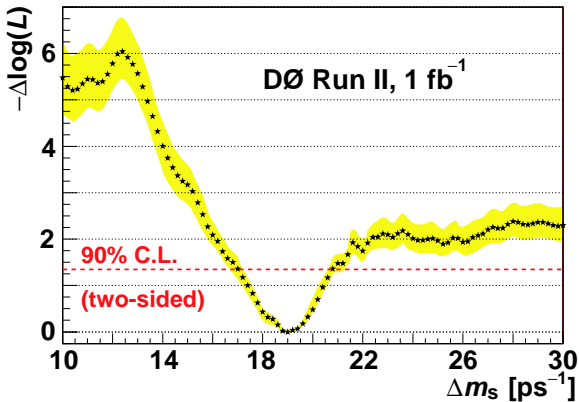
The scan shown in Fig. 8 is obtained when the method is applied to  $B_d^0 \rightarrow J/\psi K^{*0}$  and  $B_d^0 \rightarrow D^- \pi^+$  samples from the CDF experiment, using the combined opposite-side tagging algorithms. The expected compatibility of the measured amplitude with unity in the vicinity of the true frequency,  $\Delta m_d = 0.5 \text{ ps}^{-1}$ , is verified.

## 4.7. DØ $\Delta m_s$ Results

The DØ amplitude scan on  $1 \text{ fb}^{-1}$  is shown in Fig. 9. The sensitivity is  $14.1 \text{ ps}^{-1}$ , and the 95% C.L. limit is  $\Delta m_s > 14.8 \text{ ps}^{-1}$ . Fig. 10 shows the ratio of the likelihood function at  $\mathcal{A} = 0$  and  $\mathcal{A} = 1$ . The preferred value assuming a signal is  $\Delta m_s = 19 \text{ ps}^{-1}$ , with a 90% C.L. interval of  $17 < \Delta m_s < 21 \text{ ps}^{-1}$ . The probability that the random-tag background could fluctuate to mimic such a signature is about 5%.

## 4.8. CDF $\Delta m_s$ Results

The CDF combined amplitude scan on  $1 \text{ fb}^{-1}$  is shown in Fig. 11. The sensitivity for the combination

Figure 8:  $\Delta m_d$   $\mathcal{A}$ -scan in hadronic decays (CDF).Figure 11:  $\Delta m_s$   $\mathcal{A}$ -scan (CDF). The dotted line represents  $1.645\sigma_{\mathcal{A}}$ , indicating a sensitivity of  $\Delta m_s = 25.8 \text{ ps}^{-1}$ .Figure 9:  $\Delta m_s$   $\mathcal{A}$ -scan (DØ). The dotted line represents  $1.645\sigma_{\mathcal{A}}$ , indicating a sensitivity of  $\Delta m_s = 14.1 \text{ ps}^{-1}$ .Figure 10: Value of  $-\Delta\mathcal{L}$  as a function of  $\Delta m_s$  (DØ). The shaded band represents the envelope of all  $\log \mathcal{L}$  scan curves due to different systematic uncertainties.

of all hadronic and semileptonic modes is  $25.8 \text{ ps}^{-1}$ , and the 95% C.L. limit is  $\Delta m_s > 16.7 \text{ ps}^{-1}$ .

The amplitude shows a value consistent with unity near  $\Delta m_s = 17.3 \text{ ps}^{-1}$ . To assess the significance of this deviation, CDF looked at the ratio of the likelihood function at  $\mathcal{A} = 0$  and  $\mathcal{A} = 1$ , as shown in Fig. 12. The maximum likelihood ratio is at  $\Delta m_s = 17.3 \text{ ps}^{-1}$  and has an absolute value of 6.75. The probability that the random-tag background could fluctuate to mimic such a signature is 0.2%. Under the hypothesis that this is a signal for  $B_s^0 - \bar{B}_s^0$  oscillations, CDF measures

$$\Delta m_s = 17.31_{-0.18}^{+0.33} (\text{stat.}) \pm 0.07 (\text{syst.}) \text{ ps}^{-1},$$

with the systematic error completely dominated by the time scale uncertainty, which is 0.4%.

## 5. Conclusions

Lifetime measurements have been made in the clean  $\Lambda_b^0 \rightarrow J/\psi \Lambda^0$  decay. The CDF result is the most precise measurement of  $\tau(\Lambda_b^0)$ , and the first using a fully reconstructed mode that reaches a precision comparable with the previous best measurements based upon semileptonic decays of the  $\Lambda_b^0$ . Both DØ and CDF have measured the width difference between the light and heavy  $B_s^0$  mass eigenstates, which, in the limit of no  $CP$  violation, coincide with the  $CP$ -even and  $CP$ -odd eigenstates of the  $B_s^0$  system.

DØ has performed a study of  $B_s^0 - \bar{B}_s^0$  oscillations using  $B_s^0 \rightarrow \mu^+ D_s^- X$  decays and opposite-side flavor tagging algorithms. The expected limit at 95% C.L. is  $14.1 \text{ ps}^{-1}$ . Assuming Gaussian uncertainties, a 90% C.L. interval of  $17 < \Delta m_s < 21 \text{ ps}^{-1}$  is set.

CDF has searched for  $B_s^0$  flavor oscillations using hadronic and semileptonic decays. Opposite-side and, for the first time at a hadron collider, same-side tags

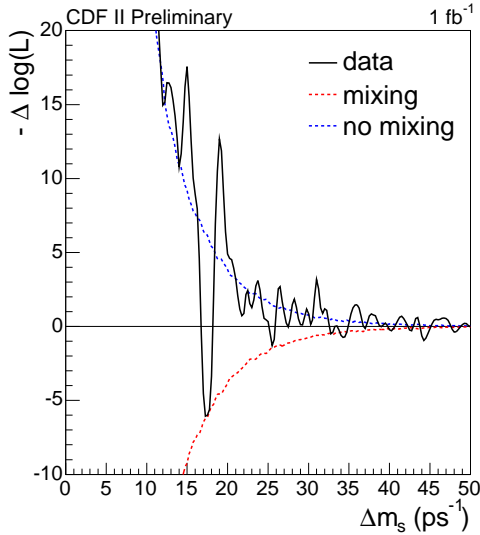


Figure 12: Combined likelihood ratio as a function of  $\Delta m_s$  (CDF).

provide information about the  $B_s^0$  production flavor. A significant peak in the amplitude scan consistent with unity is observed. Assuming this is a signal for  $B_s^0 - \bar{B}_s^0$  oscillations, CDF measures

$$\Delta m_s = 17.31_{-0.18}^{+0.33} \text{ (stat.)} \pm 0.07 \text{ (syst.) ps}^{-1}.$$

The  $B_s^0 - \bar{B}_s^0$  oscillation frequency measured at CDF is used to derive the ratio  $|V_{td}/V_{ts}|$ ,

$$\begin{aligned} \left| \frac{V_{td}}{V_{ts}} \right| &= \xi \sqrt{\frac{\Delta m_d M_{B_s^0}}{\Delta m_s M_{B_d^0}}} \\ &= 0.208_{-0.002}^{+0.001} \text{ (exp.)} {}_{-0.006}^{+0.008} \text{ (theo.)}, \end{aligned}$$

where the following values have been used as inputs:  $M_{B_d^0}/M_{B_s^0} = 0.98390$  [5] with negligible uncertainty,  $\Delta m_d = 0.505 \pm 0.005 \text{ ps}^{-1}$  [5] and  $\xi = 1.21_{-0.035}^{+0.047}$  [18].

## Acknowledgments

We would like to thank the Local Organizing Committee for a very enjoyable conference, and for accom-

modating the request for an extra talk on  $B_s^0$  mixing at CDF.

J. Piedra is supported by the EU funding under the RTN contract: HPRN-CT-2002-00292, Probe for New Physics.

## References

- [1] A. Abachi *et al.*, FERMILAB-PUB-96-357-E.
- [2] R. Blair *et al.*, FERMILAB-PUB-96-390-E.
- [3] T. Becher, FERMILAB-CONF-04-309-T; C. Tarantino, hep-ph/0310241; E. Franco, V. Lubicz, F. Mescia, C. Tarantino, Nucl. Phys. B **633** 212, hep-ph/0203089; F. Gabbiani, A. I. Onishchenko, A. A. Petrov, Phys. Rev. D **70** 094031, hep-ph/0407004; M. Beneke, G. Buchalla, C. Greub, A. Lenz, U. Nierste, Nucl. Phys. B **639** 389, hep-ph/0202106.
- [4] Heavy Flavor Averaging Group, hep-ex/0603003; F. Gabbiani, A. I. Onishchenko, A. A. Petrov, Phys. Rev. D **68** 114006, hep-ph/0303235.
- [5] S. Eidelman *et al.*, Phys. Lett. B **592** 1.
- [6] V. M. Abazov *et al.*, hep-ex/0604046, submitted to Phys. Rev. Lett.
- [7] A. Dighe *et al.*, Phys. Lett. B **369** 144.
- [8] T. Affolder *et al.*, Phys. Rev. Lett. **85** 4668; V. M. Abazov *et al.*, Phys. Rev. Lett. **95** 171801.
- [9] D. Acosta *et al.*, Phys. Rev. Lett. **94** 101803.
- [10] DØ Conference Note 5052.
- [11] A. Lenz, hep-ph/0412007; M. Beneke, G. Buchalla, C. Greub, A. Lenz, U. Nierste, Phys. Lett. B **459** 631, hep-ph/9808385.
- [12] D. Tonelli, FPCP 2006 Proceedings, fpcp06\_112, hep-ex/0605038.
- [13] R. Van Kooten, FPCP 2006 Proceedings, fpcp06\_342, hep-ex/0606005.
- [14] V. M. Abazov *et al.*, hep-ex/0603029, accepted for publication in Phys. Rev. Lett.
- [15] [www-cdf.fnal.gov/physics/new/bottom/bottom.html](http://www-cdf.fnal.gov/physics/new/bottom/bottom.html).
- [16] T. Sjöstrand, Comp. Phys. Commun. **135** 238.
- [17] H. G. Moser, A. Roussarie, NIM A384, 491-505.
- [18] M. Okamoto, hep-lat/0510113.